

## Interplay between demixing and freezing in two-dimensional symmetrical mixtures

A. Patrykiewicz\* and S. Sokołowski

*Department for the Modelling of Physico-Chemical Processes, Faculty of Chemistry, MCS University, 20031 Lublin, Poland*

(Received 16 November 2009; published 15 January 2010)

The interplay between demixing and freezing in two-dimensional symmetrical binary mixtures of Lennard-Jones particles is studied using Monte Carlo simulation. It is demonstrated that different scenarios are possible. For example, the line of continuous liquid demixing transition can start at the liquid side of the vapor-liquid coexistence at the lower critical end point and then it can terminate at the liquid side of the liquid-demixed solid coexistence at the upper critical end point. Other situations are also possible. We distinguish four different scenarios depending on the interactions between unlike particles.

DOI: [10.1103/PhysRevE.81.012501](https://doi.org/10.1103/PhysRevE.81.012501)

PACS number(s): 64.75.Ef, 47.51.+a, 61.20.Ja

Symmetrical binary mixtures (SBMs) have been intensively studied over many years [1–12] and still their phase behavior is not fully understood. A vast majority of efforts has been devoted to the understanding of phase separation in fluids, while the formation of solid phases has not been studied in detail. Binary mixtures are known to form different solidlike phases including mixed solid solutions, glasses, and crystals [13–15]. Freezing also leads to a phase separation and the formation of crystallites of pure components. In fact, crystallization is one of the methods used to separate enantiomers [16] and the symmetrical mixture is simple and yet quite reasonable model for racemic mixtures.

Thermodynamics of a SBM can be conveniently described using grand canonical ensemble and its phase diagram is spanned by three thermodynamic fields: the temperature  $T$  and the chemical potentials  $\mu_A$  and  $\mu_B$ . Under the assumed here condition of  $\mu_A = \mu_B = \mu$ , the chemical potential  $\mu$  is coupled to the total density  $\rho = \rho_A + \rho_B$  and the ordering field  $h = \mu_A - \mu_B = 0$ . Both  $\rho_A$  and  $\rho_B$  are on average the same, though they are allowed to fluctuate. Of course, in finite systems studied by computer simulation methods, demixing in the system may lead to large density differences due to metastability effects and finite “observation time.”

As long as fluid phases are concerned, the phase diagram topologies of SBMs have been classified into different categories depending on the tendency of the system to phase separate [5,6,10]. A detailed discussion of different possible situations can be found in Refs. [6,10]. However, the question of a possible interplay between demixing and freezing transitions in SBMs has not been answered so far. This is an interesting problem and the aim of this work is to study it using Monte Carlo simulations. The obtained results should enrich our knowledge about possible phase diagram categories of SBMs. They might also be useful for experimentalists helping to construct experimental setups for effective phase separation of binary mixtures.

We consider a simple model of two-dimensional SBMs interacting via the Lennard-Jones (LJ) potentials

$$u_{ij}(r) = 4\varepsilon_{ij}[(\sigma_{ij}/r)^{12} - (\sigma_{ij}/r)^6]. \quad (1)$$

For SBMs, we have  $\varepsilon_{AA} = \varepsilon_{BB} = \varepsilon$  and  $\sigma_{AA} = \sigma_{BB} = \sigma$ . Throughout this work, we take  $\varepsilon$  and  $\sigma$  as units of energy and length,

respectively. The corresponding potential parameters for  $AB$  interaction are  $\varepsilon_{AB} = e\varepsilon$  and  $\sigma_{AB} = s\sigma$ . The magnitudes of both  $e$  and  $s$  determine the phase behavior of SBMs [6]. In particular, when  $e < 1$ , the system is expected to phase separate at sufficiently low temperatures and at sufficiently high densities.

All the calculations reported here were carried out for a special case of  $h=0$  (or  $\mu_A = \mu_B$ , which implies that  $\rho_A = \rho_B = \rho/2$  in the mixed phase). To construct a full phase diagram, the consideration of the cases of  $h \neq 0$  is obviously necessary. However, even the case considered here might be interesting because a number of important systems, as a mixture of  $\text{He}^3$  and  $\text{He}^4$  or ferroelectric liquids, can be mapped onto it.

For certain range of  $e$  and  $s$ , the line of a continuous demixing transition (the  $\lambda$  line) meets the liquid side of the first-order vapor-liquid phase boundary at the critical end point ( $T_{cep}$ ), below the vapor-liquid critical point,  $T_c$ . At  $T_{cep}$ , a critical liquid coexists with a noncritical vapor. Locations of both  $T_{cep}$  and  $T_c$  depend on the parameters  $e$  and  $s$ . For a fixed  $s$ , a decrease of  $e$  leads to a gradual increase of the tendency toward phase separation and hence  $T_{cep}$  increases, while the critical point temperature is expected to decrease when  $e$  becomes lower. We also know that when  $e$  becomes sufficiently small, the phase diagram topology changes and the vapor-mixed liquid critical point is replaced by the tricritical point in which the vapor,  $A$ -rich and  $B$ -rich liquid phases all become critical [6]. The temperature of demixing transition depends on the density, so that one has a critical line of consolute points  $T_\lambda(\rho)$  [or  $T_\lambda(\mu)$ ] and  $T_\lambda$  increases with  $\rho$ .

The mixture also exhibits solid phases at sufficiently low temperatures, as well as at sufficiently high densities. Now, we would like to discuss different scenarios involving the interplay between demixing and fluid-solid transitions.

Of course, when the temperature becomes lower than the vapor-liquid-solid triple-point temperature,  $T_{tr}$ , the vapor-solid transition takes place and the resulting solid can be either mixed or demixed depending on the magnitudes of the parameters  $e$  and  $s$ . For  $e < 1$ , the solid phase is bound to be demixed at sufficiently low temperatures. Moreover, the triple-point temperature also depends on the magnitudes of  $e$  and  $s$ .  $T_{tr}$  should converge to the triple-point temperature of one-component LJ system when the mixture exhibits sufficiently strong tendency toward phase separation and should

\*andrzej@pluto.umcs.lublin.pl

decrease upon the increase of  $e$  due to large entropic effects. At the temperatures above  $T_{lr}$ , the fluid-solid transition and the structure of resulting solid phase both depend on the properties of a fluid at the fluid-solid coexistence and different situations can appear depending on the behavior of  $\lambda$  line and the location of the critical end point of the demixing transition.

There are two main factors influencing the interplay between demixing and freezing. One is the relative slope of the  $\lambda$  line [ $\delta_\lambda = dT_\lambda(\rho)/d\rho$ ] and the density derivative of the freezing temperature (liquid side of the liquid-solid coexistence),  $\delta_f$ . The second is the locus of the critical end point of demixing transition with respect to the triple point.

One can single out two different scenarios solely considering the magnitudes of  $\delta_\lambda$  and  $\delta_f$ . When  $\delta_\lambda > \delta_f$  (the case I), the system can exhibit only one critical end point, which, however, can be located either at the liquid side of the vapor-liquid coexistence (case Ia) or at the liquid side of the liquid-solid coexistence (case Ib). Of course, there must exist a special case when  $T_{cep} = T_{lr}$  and  $\rho_{cep} = \rho_{lr}$ , i.e., the critical end point and triple point merge into a multicritical point.

On the other hand, when  $\delta_\lambda < \delta_f$  (the case II), one expects to observe two (lower and upper) critical end points ( $T_{l,cep}$  and  $T_{u,cep}$ ) (case IIa) or no critical end points at all (case IIb). When two critical end points occur, then the lower is located at the liquid side of the vapor-liquid coexistence, while the upper at the liquid side of the liquid-solid coexistence. This situation occurs whenever  $T_{l,cep} > T_{lr}$ . Then it is expected to observe the transition between demixed solid (stable at low temperatures) and mixed solid (stable at high temperatures).

Below, using computer simulations, we shall demonstrate that the cases I and II do exist in the model considered. Explicit Monte Carlo calculations in the grand canonical ensemble [17,18] (for the special case of  $\mu_A = \mu_B$ ) have been carried out for two series of systems with the fixed values of  $s$  equal to 1.0 and 1.24, while the parameter  $e$  has been varied in both series. The interaction potential was cut at the distance equal to  $3\sigma$  and square simulation cells of the size  $L \times L$ , with  $L$  ranging between 20 and 40, with periodic boundary conditions were used. We have recorded the densities of both components, the order parameter

$$m = (N_A - N_B)/(N_A + N_B), \quad (2)$$

being the measure of phase separation in the system, as well as the corresponding susceptibilities allowing to monitor fluctuations of the total density of the densities of both components and of the above-defined order parameter. In some cases, we have also determined the distribution functions of the total density and of the order parameter  $m$ . Distribution functions have been evaluated using hyperparallel tempering method [19]

Figure 1 presents the examples of phase diagrams (in the  $T$ - $\rho$  plane) obtained for the systems characterized by  $e=0.7$  and different values of  $s=1.24$  (part a) and 1.00 (part b). It is evident that these phase diagrams have the same topologies as described by the cases (Ib) and (IIa), respectively.

From the results given in Fig. 1(a), we learn that the system corresponds to the case (Ib). The estimated critical and

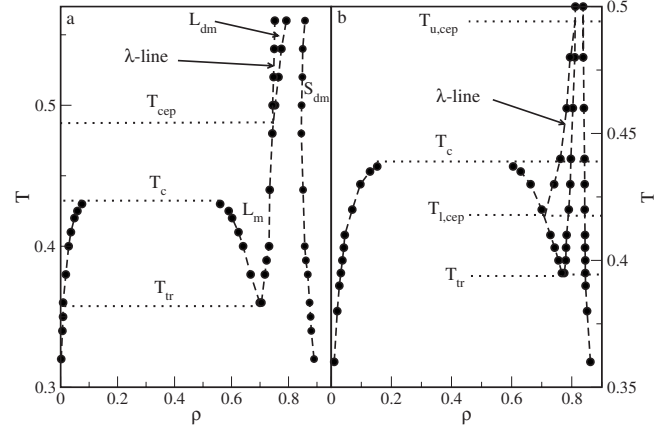


FIG. 1. The phase diagrams (in the  $T$ - $\rho$  plane) for the system (a) with  $e=0.7$  and  $s=1.24$  and (b) with  $e=0.7$  and  $s=1.0$ . In (a), the symbols V, L, and S denote vapor, liquid, and solid phases, respectively, while the subscripts m and dm refer to mixed and demixed phases, respectively.

triple-point temperatures, equal to about 0.43 and 0.35, respectively, are both lower than the corresponding values for one-component LJ system [20]. For the chosen value of  $e$ , the  $\lambda$ -line starts already at the liquid-solid coexistence at  $T_{cep} \approx 0.485$ . However, for the system depicted in Fig. 2(b), the topology of the phase diagram is different and corresponds to the case (IIa). The critical temperature, equal to about 0.44, is only slightly different from that for the system with  $s=1.24$ . This result is rather obvious, since in mixed

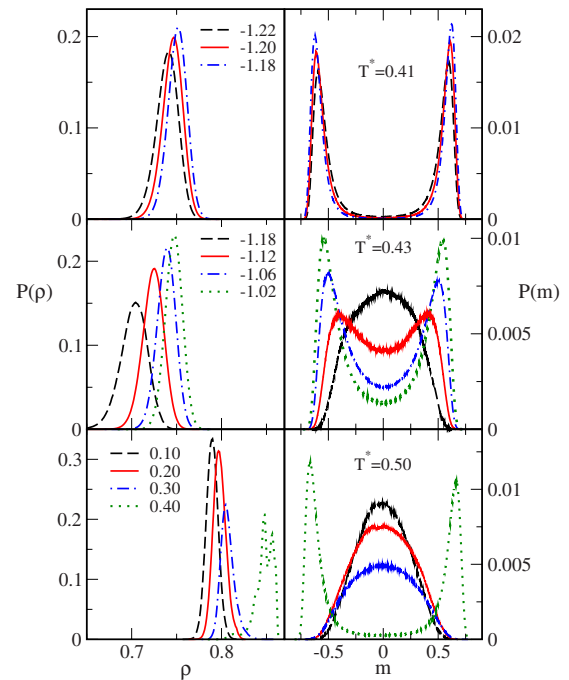


FIG. 2. (Color online) Histograms of density (left panels) and of the order parameter  $m$  (right panels) for the systems just below the  $T_{l,cep}$  (upper panel), at  $T_{l,cep} < T < T_{u,cep}$  (middle panels), and just above  $T_{u,cep}$  (lower panels). The temperatures are given in right panels, while the numbers in the left panels give the values of the chemical potential,  $\mu$  (in the units of  $\epsilon$ ).

liquids the differences due to packing effects are not important. On the other hand, the triple-point temperature, equal to about 0.39, is quite close to the triple point temperature of one-component LJ system. One should note that at  $T_{tr}$ , the solid forms from already demixed liquid.

For the system with  $s=1.0$ , the triple-point density is quite close to the triple-point density of one-component LJ system, while in the case of  $s=1.24$  it is considerably lower due to packing effects. This large difference in triple-point densities causes that the  $\lambda$  line starts at the densities below (for  $s=1.0$ ) and above (for  $s=1.24$ ) the triple-point density. As Fig. 1(b) shows, the system with  $s=1.0$  exhibits two, lower and upper, critical end points of liquid demixing transition, equal to  $T_{l,cep} \approx 0.418$  and  $T_{u,cep} \approx 0.495$ .

The appearance of demixing transition was verified by examination of the distributions of the order parameter  $m$ . Figure 2 gives representative examples obtained for the system from Fig. 1(b) ( $s=1.0$  and  $e=0.7$ ). Left (right) panels show the density (order-parameter) distributions obtained at the temperatures below  $T_{l,cep}$  (upper panels), in between  $T_{l,cep}$  and  $T_{u,cep}$  (middle panels), and above  $T_{u,cep}$  (lower panels). Upper panels correspond to the demixed liquid phase at the chemical potentials just above vapor-liquid coexistence point ( $\mu_{coex} \approx -1.245$ ), so that we are below the lower critical end point. Middle panels also show the liquid above the vapor-liquid coexistence ( $\mu_{coex} \approx -1.225$ ), but evidently above  $T_{l,cep}$  and demonstrate the existence of demixing transition. The histogram of  $m$  at  $\mu = -1.18$  shows a mixed phase while the histograms for  $\mu \geq -1.12$  show already demixed liquid. The left lower panel illustrates the liquid-solid transition at  $T=0.50$ . Of course, grand canonical simulations are not well suited to sample solid phases, one should rather use the NPT ensemble. Therefore, it is not surprising that the density histogram for a solid phase possesses a multippeak structure. It should be stressed, however, that the order-parameter histograms demonstrate that the liquid is mixed while the solid is demixed. Therefore, this situation corresponds to the temperature above the upper critical end point. Quite similar results have been obtained for other systems considered, but for the sake of brevity, we do not present them here.

From the phase diagrams obtained for different values of the parameters  $e$  and  $s$ , we have estimated the locations of characteristic points involving the critical point of the vapor-liquid transition, critical end points of the fluid demixing transition, as well as triple points. Then, we have collected the results plotting the values of those characteristic temperatures versus  $e$ , keeping the parameter  $s$  fixed. Part a of Fig. 3 collects the results obtained for the systems characterized by  $s=1$ , while part b the results obtained for  $s=1.24$ .

The results shown in Fig. 3(a) confirm the predictions concerning the appearance of two, lower and upper, critical end points in the case of mixtures in which the  $\lambda$ -line exhibits strong density dependence. It also shows that the multicritical point (marked by filled square, and additionally abbreviated as  $T_m$ ) does exist for  $e \approx 0.745$ . Moreover, it is seen that the triple-point temperature gradually approaches the triple-point temperature of one-component LJ fluid when the parameter  $e$  decreases. Our results suggest that for  $e > 0.66$ , the vapor-liquid transition terminates in the critical points,

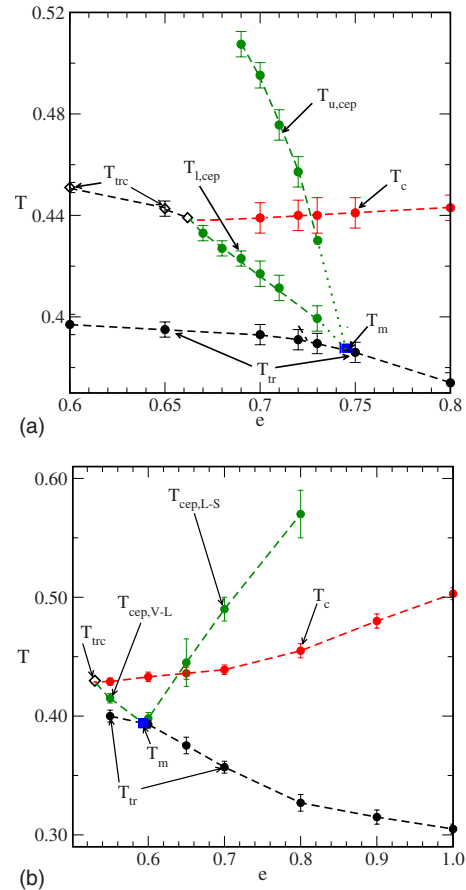


FIG. 3. (Color online) The changes of critical, triple-point, and critical end point temperatures with the parameter  $e$  for the systems characterized by (a)  $s=1.0$  and (b)  $1.24$ .

$T_c$ . However, explicit Monte Carlo results for  $e=0.6, 0.65$ , and  $0.66$  have demonstrated that vapor-liquid transition terminates at the tricritical rather than at the critical point,  $T_{trc}$ . Tricritical points are shown as open diamonds in Fig. 3. For  $e$  up to  $0.73$ , the solid phase was demixed over the entire range of temperatures used. For higher values of  $e=0.75$  and  $0.80$ , we have observed the demixing solid-solid transition. In the case of  $e=0.75$ , the solid phase was found to be demixed at the temperatures below about  $0.44$  and mixed at higher temperatures. In the case of  $e=0.8$ , this demixing transition occurs at considerably lower temperature. At  $T=0.34$ , we have found demixed solid while at  $T=0.38$ , the solid was already mixed. Extremely large metastability effects excluded any possibility to locate the transition points with a considerable accuracy. One can also expect that the transition between demixed and mixed solid phases occurs in the systems with lower values of the parameter  $e$ , but at higher temperatures than used here.

For the systems with  $s=1.24$  [Fig. 3(b)] the  $\lambda$  line shows a weak density dependence and the phase diagrams such as that depicted in Fig. 1(a) were found. For small  $e$ , the critical end point is located at the liquid side of the vapor-liquid coexistence, leading to the phase diagram topology described as the case Ia. The crossover between the cases Ia and Ib occurs at the multicritical point,  $T_m$ , located at  $T_m \approx 0.59$ , as indicated by a filled square in Fig. 3(b). For the values of  $e$

lower than 0.59, the critical end points are located at the liquid side of the vapor-liquid coexistence envelope (the line abbreviated as  $T_{cep,v-L}$ ), otherwise it is located at the liquid side of the liquid-solid coexistence line [the line abbreviates as  $T_{cep,L-S}$  in Fig. 3(b)]. Moreover, for  $e$  below about 0.525, one also expects the appearance of tricritical point instead of the vapor-liquid critical point. It should be also noted that the solid phase is demixed over the entire range of temperatures studied.

The results reported here indicate the necessity to calculate complete phase diagrams of SBMs, involving fluid-solid transitions in order to categorize them into relevant classes. Different interplay between demixing and freezing transitions may lead to qualitative changes of the phase diagram topology.

This work was supported by Polish Ministry of Science under Grant No. N N202 046137.

- 
- [1] J. S. Rowlinson and F. L. Swinton, *Liquids and Liquid Mixtures*, 3rd ed. (Butterworths, London, 1982).
- [2] A. Z. Panagiotopoulos, N. Quirke, M. Stapleton, and D. J. Tildesley, *Mol. Phys.* **63**, 527 (1988).
- [3] E. de Miguel, E. M. del Rio, and M. M. Telo da Gama, *J. Chem. Phys.* **103**, 6188 (1995).
- [4] N. B. Wilding, *Phys. Rev. Lett.* **78**, 1488 (1997).
- [5] N. B. Wilding, *Phys. Rev. E* **55**, 6624 (1997).
- [6] N. B. Wilding, F. Schmid, and P. Nielaba, *Phys. Rev. E* **58**, 2201 (1998).
- [7] G. Kahl, E. Schöll-Paschinger, and A. Lang, *Monatsh. Chem.* **132**, 1413 (2001).
- [8] E. Schöll-Paschinger, D. Levesque, J.-J. Weis, and G. Kahl, *Phys. Rev. E* **64**, 011502 (2001).
- [9] D. Woywod and M. Schoen, *Phys. Rev. E* **73**, 011201 (2006).
- [10] J. Köfinger, N. B. Wilding, and G. Kahl, *J. Chem. Phys.* **125**, 234503 (2006).
- [11] E. Diaz-Herrera, G. Ramirez-Santiago, and J. A. Moreno-Razo, *J. Chem. Phys.* **123**, 184507 (2005).
- [12] S. K. Das, J. Horbach, K. Binder, M. E. Fisher, and J.-V. Sengers, *J. Chem. Phys.* **125**, 024506 (2006).
- [13] M. J. Vlot and J. P. van der Eerden, *J. Chem. Phys.* **109**, 6043 (1998).
- [14] M. R. Hitchcock and C. K. Hall, *J. Chem. Phys.* **110**, 11433 (1999).
- [15] B. Coluzzi, M. Mézard, G. Parisi, and P. Verrocchio, *J. Chem. Phys.* **111**, 9039 (1999).
- [16] J. Jacques, A. Collet, and S. H. Wilen, *Enantiomers, Racemates and Resolutions* (Krieger, Malabar, 1991).
- [17] M. P. Allen and D. J. Tildesley, *Computer Simulation of Liquids* (Oxford University Press, Oxford, 1987).
- [18] D. P. Landau and K. Binder, *A Guide to Monte Carlo Simulation in Statistical Physics* (Cambridge University Press, Cambridge, England, 2000).
- [19] Q. Yan and J. J. de Pablo, *J. Chem. Phys.* **111**, 9509 (1999).
- [20] F. F. Abraham, *Phys. Rep.* **80**, 340 (1981).